7th World Congress on Civil, Structural, and Environmental Engineering (CSEE'22)
~~Lisbon, Portugal~~ Virtual Conference – April 10 – 12, 2022
Paper No. ICSECT 127
DOI: 10.11159/icsect22.127

A Vision-Based System for Structural Displacement Measurement

Felipe J. Perez[1], Omar E. Mora[1]
[1]California State Polytechnic University, Pomona
3801 West Temple Ave., Pomona, CA, U.S.A.
fperez@cpp.edu; oemora@cpp.edu

Abstract **–** Current structural displacement measurement methods for structural health monitoring (SHM) are based on displacement data of acceleration, strain, laser doppler vibrometer, Light Detection and Ranging (LiDAR), total station, and Global Navigation Satellite System (GNSS) measurements. However, these methods are time consuming, labor intensive, limited in spatial and temporal resolution, costly and restricted to certain applications. For these reasons, a new method to measure structural displacements is needed. This study examines a novel structural displacement measurement method using a vision-based system coupled with computer vision algorithms. To test and evaluate the performance of the proposed method, seven tests were performed with varying focal lengths and 89 distance measurements using a calibrated meter stick. Results show that the error in a distance measurement decreases to within 0.02% as the measured distance increases for a fixed focal length. Furthermore, the error in a distance measurement decreases to within 1.15% as the focal length increases. Therefore, the proposed methodology is recommended for efficiently measuring structural displacements ranging from 1 mm to 1000 mm with errors less than 1.15%.

Keywords**:** Computer vision, Structural Health Monitoring, Displacement measurement

1. Introduction

Structural displacement measurements are critical for structural health monitoring (SHM). They support civil infrastructure evaluations related to performance, safety, and serviceability [1]. Current structural displacement measurement data for SHM can be obtained from accelerometers, Global Navigation Satellite System (GNSS), laser doppler vibrometer, Light Detection and Ranging (LiDAR), strain and total station measurements [2]. However, these methods are time consuming, labor intensive, limited in spatial and temporal resolution, costly and restricted to certain applications [1-2].

In the last decade, the advancements made in SHM technology have improved in spatial and temporal resolution, efficiency, and cost-effectiveness [3-6]. Although prior studies have devoted considerable contributions to developing a novel sensing system using state-of-the-art SHM technology, current approaches are limited to being contact based, thus restricting their application and feasibility [7-8]. Structural displacement measurements are critical in safeguarding engineering structures, particularly, to assess their condition, performance, inspection, and maintenance for operational safety [1]. For these reasons, a novel sensing system to measure structural displacements for SHM is needed.

The advancements made in vision-based systems, computer science, hardware, software, and automated algorithms provide a unique opportunity to develop a new technique for measuring structural displacements [2]. In particular, the improvements made in vision-based systems coupled with computer vision algorithms provide new opportunities for collecting, processing, and analysing structural displacement data [3-6]. Vision-based systems fused with computer vision algorithms provide unique advantages for noncontact, long distance, high precision, high temporal and spatial resolution data for structural displacement measurements and monitoring [3-8].

Currently, many vision-based systems coupled with computer vision algorithms have been developed for structural displacement measurement for SHM [3-8]. Applications include crack/defect inspection, characterization, strain/stress monitoring, and vibration response monitoring, to name a few [3-11]. Ongoing developments for SHM are based on close-range photogrammetry for deformation measurements of bridges and buildings [1-11]. Other studies focus on structural defect analysis of asphalt and concrete, including their detection and condition assessment [9-11]. Although the results from prior studies are promising, a study focused on the performance of a vision-based sensing system coupled with computer vision algorithms is not well understood.

In this study, the results of an experimental study to develop, calibrate, implement, and evaluate the likelihood of a novel vision-based sensing system coupled with computer vision algorithms for obtaining structural displacement measurements for SHM of civil infrastructure systems is shown. Measurements are obtained by using a digital camera in conjunction with computer vision algorithms to measure distances on a calibrated meter stick. Subsequently, the distances are compared to their actual distance and a percent error is computed. The results show that a vision-based system and the proposed computer vision methodology is robust for obtaining noncontact measurements with an observed percent error less than 1.15% for measurements ranging from 1 to 1000 mm.

2. Methodology

A new vision-based sensing system coupled with computer vision algorithms for structural displacement measurements is proposed. The suggested methodology is summarized in Fig. 1 and consists of the image acquisition system (digital camera and lens), software for processing the imagery (typically built-in to the digital camera), a structure, targets mounted on the structure where displacement measurements are required, hardware to perform computations (computer) and the computer vision algorithm (software code). In this section, the concept and the principle of the proposed method is described.

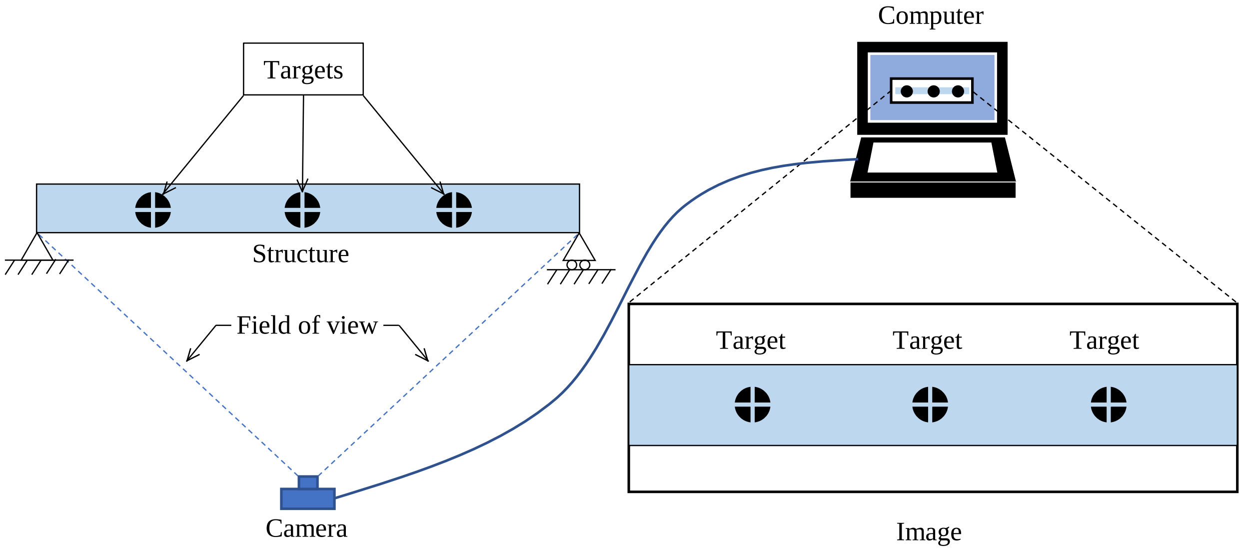

Fig. 1: Two-dimensional vision-based structural displacement measurement method.

2.1. Vision-Based System & Image Acquisition

The proposed vision system consists of a camera, zoom lens and an image processor. The setup consists of a digital camera being set on a tripod and placed at a fixed location away from the specimen being analyzed. The camera is thus set to have a fixed focal length. Then, the image data is collected using a remote trigger. Finally, the camera is connected to a computer, where the distance measurements are performed using a computer vision algorithm. It is noted that setting up the vision system, collecting the data and performing the distance measurements only takes a few minutes.

2.2. Scale Factor

The structural displacement measurements are initially measured in pixels. However, to obtain engineering displacement measurements, it is necessary to convert the distance measurements in the image plane to distance measurements in the object space. Therefore, a scale factor is required to perform the transformation. The scale factor in mm/pixel is defined as the transformation between the units in the image plane and the physical units. When the image plane is parallel to the object surface, the scale factor (SF) can be computed using Equation (1). It is recommended to mount a scale on the structure in the Region of Interest (ROI) to obtain an accurate scale factor.

$$SF = \frac{d_{object}}{d_{image}} \left[\frac{mm}{pixel}\right] \tag{1}$$

where, d_{object} = physical dimension of an object (mm)
d_{image} = image dimension of an object (pixel)

2.3. Computer Vision Algorithm

The computer vision algorithm shown in Fig. 2 computes the structural displacement measurement as follows. First, the image coordinates of the first frame of the target are identified, where the first frame corresponds to an unloaded structure state. Subsequently, the image coordinates of the second frame are observed, where the second frame corresponds to a loaded structure state. Next, the horizontal and vertical distance in pixels between the first and second frames are computed. Next, the horizontal and vertical distance in pixels is transformed to distance in mm by applying the scale factor per Eq. (1). Finally, the vertical and horizontal distances in mm are converted to a Euclidean distance using the Square Root of the Sum of Squares (SRSS).

3. Calibration Experiments

This section describes the calibration experiments that were carried out in this study. The objectives of these experiments are: (1) To study the efficacy of the proposed vision-based system to obtain remote linear displacement measurements; (2) To correlate the error in linear displacement measurements to the magnitude of the measured distance for various focal lengths; (3) To correlate the resolution with range for an acceptable margin of error.

3.1. Description of Experiments

The experimental setup used in this study is shown Schematically in Fig. 3. It consisted of propping a meter stick on a countertop and setting up a digital camera on a tripod 1 m away. The camera used was a Sony DSC-RX10M4 with a Zeiss Vario-Sonnar T* f/2.4-4 zoom lens. A remote shutter control was used to take all the photographs. The typical image width was 5472 pixels, while the typical image height was 3648 pixels. Comparing Fig. 1 to Fig. 3, the structure was replaced with a meter stick to test the accuracy of the proposed vision-based system. A total of seven tests were carried out at various focal lengths by adjusting the zoom setting in the camera. Specifically, the focal lengths for Test 1 through Test 7 were 10.28 mm, 13.63 mm, 24.94 mm, 39.35 mm, 56.31 mm, 130.09 mm, and 175.77 mm, respectively. For each test, the methodology presented in Fig. 2 was used, except that only one frame was used to obtain the pixel coordinates of both targets in the ROI. This was possible because the calibration study did not involve a physical movement of a structure, and thus did not require two frames to determine a target's movement. Instead, the graduations on the meter stick were used to represent targets that simulated the structural movements (referred to as a distance measurement herein). This was done to avoid errors when comparing against measurements from linear displacement sensors.

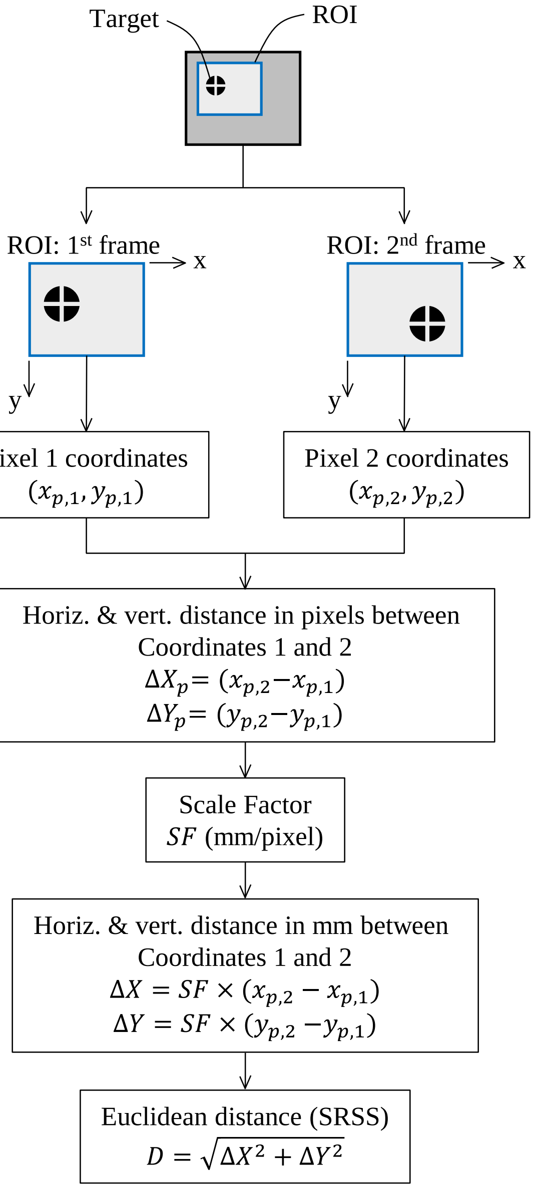

Fig. 2: Proposed vision-based sensing methodology.

For each test (i.e., for each focal length), multiple distance measurements (relative to a common reference target) were taken across the portion of the meter stick that was in view. By obtaining various distance measurements, the accuracy of each measurement was evaluated against the ground truth. Test 1 had the widest field of view with a range of 1283 mm and thus was able to accommodate the most measurements. A total of 20 measurements were selected for Test 1, ranging from 1 mm to 1000 mm. Test 2, with a range of 968 mm had 19 measurements. Test 3, with a range of 529 mm, had 15 measurements. Test 4, with a range of 335 mm, had 12 measurements. Test 5, with a range of 234 mm, had 10 measurements. Test 6, with a range of 101 mm, had seven measurements. Lastly, Test 7, with a range of 75 mm, had six measurements. Therefore, this experimental study consisted of a total of 89 distance measurements.

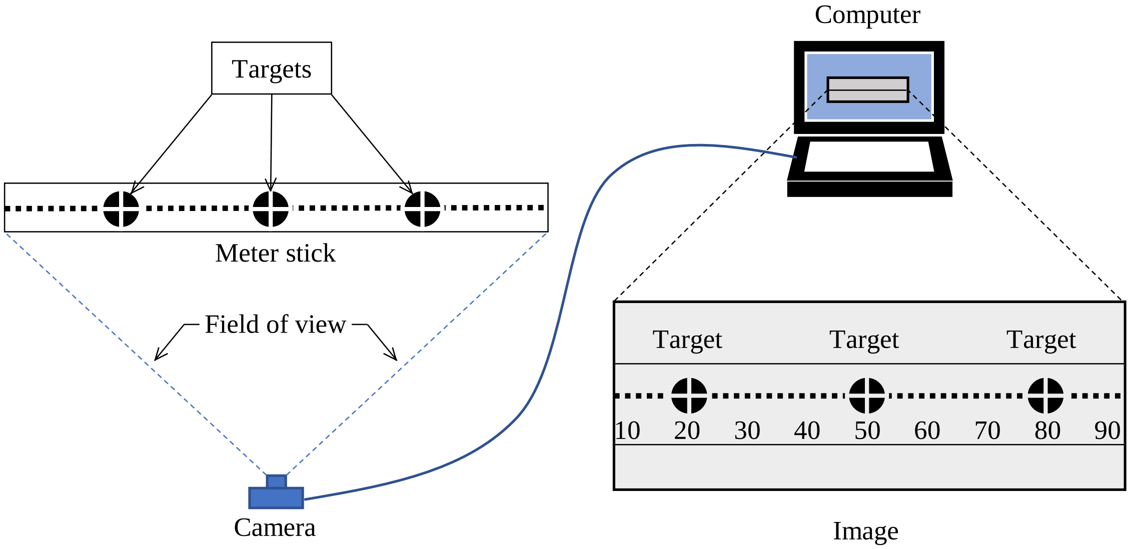

Fig. 3: Test setup used in calibration experiments.

Table 1: Summary of test results.

	Test 1		Test 2		Test 3		Test 4		Test 5		Test 6		Test 7	
Actual Dist. (mm)	Meas. Dist. (mm)	Error (%)	Meas. Dist. (mm)	Error (%)	Meas. Dist. (mm)	Error (%)	Meas. Dist. (mm)	Error (%)	Meas. Dist. (mm)	Error (%)	Meas. Dist. (mm)	Error (%)	Meas. Dist. (mm)	Error (%)
1	0.94	6.18	1.08	7.63	0.97	2.78	1.05	4.74	0.99	1.38	1.02	2.27	0.99	1.15
5	4.70	6.06	5.13	2.62	4.94	1.26	4.91	1.80	4.93	1.34	4.95	0.98	5.01	0.19
30	29.32	2.27	29.55	1.50	29.79	0.69	29.73	0.90	29.73	0.90	29.97	0.11	30.05	0.15
50	49.02	1.95	49.37	1.26	49.63	0.75	49.65	0.70	49.61	0.78	50.07	0.14	50.05	0.11
60	58.64	2.27	59.28	1.21	59.59	0.68	59.64	0.60	59.68	0.54	60.09	0.14	60.04	0.06
70	68.49	2.16	69.19	1.16	69.55	0.64	69.63	0.52	69.74	0.37	70.08	0.11	70.00	0.00
90	88.20	2.00	89.00	1.11	89.48	0.57	89.62	0.42	89.84	0.18	90.00	0.00	-	-
100	97.82	2.18	98.92	1.08	99.45	0.55	99.68	0.32	99.91	0.09	-	-	-	-
200	196.81	1.60	198.19	0.91	199.49	0.26	200.21	0.11	200.16	0.08	-	-	-	-
220	216.51	1.59	218.01	0.91	219.51	0.22	220.26	0.12	219.96	0.02	-	-	-	-
300	296.03	1.32	297.64	0.79	299.71	0.10	300.20	0.07	-	-	-	-	-	-
320	315.97	1.26	317.63	0.74	319.73	0.08	320.00	0.00	-	-	-	-	-	-
400	395.73	1.07	397.45	0.64	399.94	0.02	-	-	-	-	-	-	-	-
500	495.66	0.87	497.25	0.55	500.07	0.01	-	-	-	-	-	-	-	-
520	515.59	0.85	517.24	0.53	520.00	0.00	-	-	-	-	-	-	-	-
600	595.82	0.70	597.40	0.43	-	-	-	-	-	-	-	-	-	-
700	696.22	0.54	697.92	0.30	-	-	-	-	-	-	-	-	-	-
800	797.09	0.36	798.96	0.13	-	-	-	-	-	-	-	-	-	-
900	898.43	0.17	900.00	0.00	-	-	-	-	-	-	-	-	-	-
1000	1000.00	0.00	-	-	-	-	-	-	-	-	-	-	-	-

3.2. Results and Discussion

A total of seven tests were carried out, with various focal lengths, and multiple distance measurements for each test. Table 1 summarizes the experimental results. Up to 20 target distances were considered, ranging from 1 mm to 1000 mm, depending on the field of view range available for each test. Table 1 summarizes for each test the measured distance, based on converting pixels to linear distance measurements. In addition, the percent error relative to the actual distance is calculated for each measured distance. This error is plotted against the measured distance for all seven tests in Fig. 4. Fig. 4 and Table 1 show that the error in a distance measurement decreases to within 0.02% as the measured distance increases for a fixed focal length. When comparing all the tests, Test 1 (with a smaller focal length), resulted in greater measurement errors while Test 7, with the greatest focal length, resulted in the smallest measurement errors. Therefore, as the focal length increases (Test 1 to Test 7), the error tends to decrease. The data show that the error in a distance measurement decreases to within 1.15% as the focal length increases.

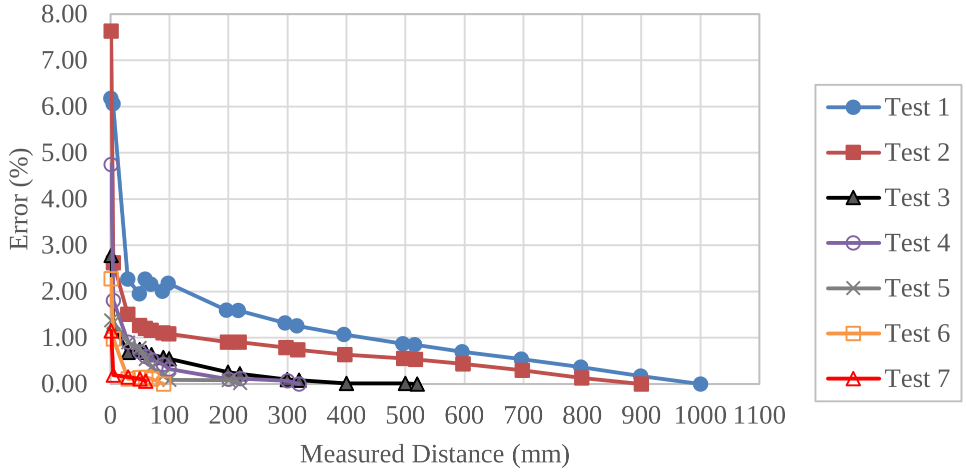

Fig. 4: Error in distance measurements for all tests.

Fig. 4 shows that consistently, the greatest error resulted for a 1 mm measurement. Fig. 5 plots the actual measurement for each test when targeting a 1 mm distance measurement. Percent errors are shown for reference. Referring to Fig. 5, when targeting a 1 mm distance, the measurement error was between 6% and 8% for Tests 1 and 2, which had the smallest focal lengths. This measurement error diminished to 1.15% for Test 7, which had the greatest focal length.

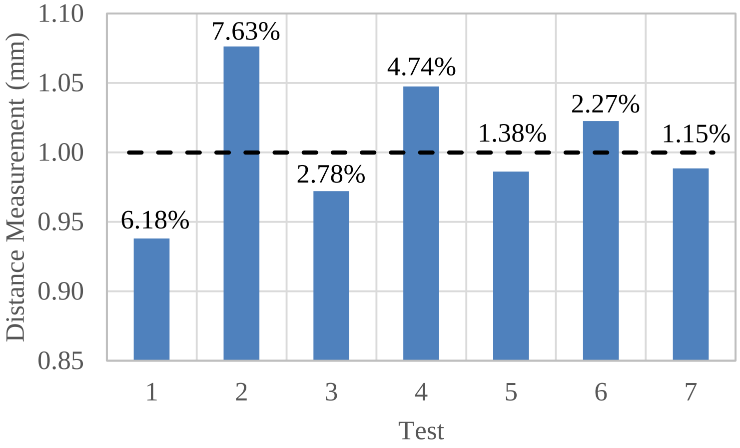

Fig. 5: Error in a 1 mm distance measurement for all tests.

It is expected that greater focal lengths result in better measurement resolution, but at the expense of a smaller field of view measurement range. Fig. 6 plots the resolution versus range for this study. The range was determined by considering the total number of pixels across each image and converting it to a distance measurement per Fig. 2, with the scale factor calculated using Eq. 1. The resolution was obtained for each test by selecting the smallest measurement with an error less than 5%. Accordingly, the data for Test 7 through Test 1 appear from left to right in Fig. 6. Test 7, with the largest focal length of 175.77 mm, had the best resolution of 1 mm with an error of 1.15%, and a range of 75.1 mm. Test 6, with a focal length of 130.09 mm, had a resolution of 1 mm with an error of 2.27%, and a range of 101.47 mm. Test 5, with a focal length of 56.31 mm, had a resolution of 1 mm with an error of 1.38%, and a range of 234.4 mm. Test 4, with a focal length of 39.35 mm, had a resolution of 1 mm with an error of 4.74%, and a range of 335.4 mm. Test 3, with a focal length of 24.94 mm, had a resolution of 1 mm with an error of 2.78%, and a range of 529.3 mm. Test 2, with a focal length of 13.63 mm, had a resolution of 5 mm with an error of 2.62%, and a range of 968.2 mm. Lastly, Test 1, with the smallest focal length of 10.28 mm, had a resolution of 30 mm with an error of 2.27%, and a range of 1283 mm. These data show that a greater range comes at the expense of loss in resolution. However, the specific values are useful in deciding the focal length needed for a given displacement measurement. A 1 mm resolution is achievable within a 5% error up to a range of 529.3 mm. Test 3, with a focal length of 24.94 mm, displayed the best combination of resolution and range (1 mm with an error of 2.78% and a range of 529.3 mm).

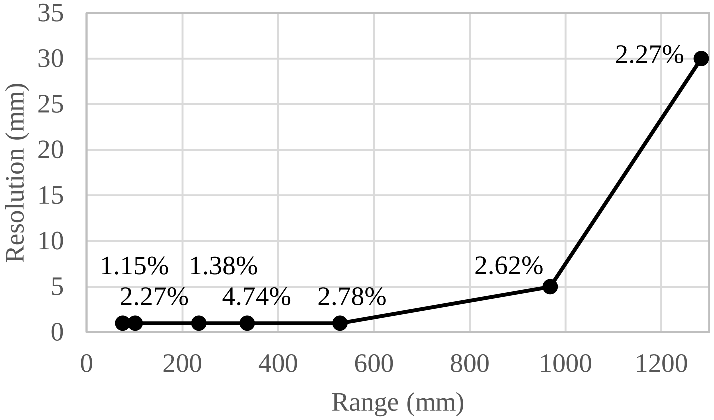

Fig. 6: Resolution vs. Range (data from Tests 7 through 1 appear from left to right).

4. Conclusion

This study examines a novel structural displacement measurement method using a vision-based system coupled computer vision algorithms. Seven tests were performed with varying focal lengths and 89 distance measurements using calibrated meter stick. The objectives of these experiments are: (1) To study the efficacy of the proposed vision-based to obtain remote linear displacement measurements; (2) To correlate the error in linear displacement measurements to magnitude of the measured distance for various focal lengths; and (3) To correlate the resolution with range for an acceptable margin of error. The following conclusions can be drawn based on this study: (1) The error in a distance measurement decreases to within 0.02% as the measured distance increases for a fixed focal length; (2) The error in a distance measurement decreases to within 1.15% as the focal length increases; (3) Test 3, with a focal length of 24.94 mm, displayed the best combination of resolution and range (1 mm with an error of 2.78% and a range of 529.3 mm); and (4) The proposed methodology is recommended for efficiently measuring structural displacements ranging from 1 mm to 1000 mm with errors less than 1.15%.

Acknowledgements

The authors want to thank the Special Projects for Improving the Classroom Experience (SPICE) Program at California State Polytechnic University, Pomona for funding the equipment utilized in this study.

References

[1] Ye, X.W., Ni, Y.Q. and Yin, J.H., 2013. Safety monitoring of railway tunnel construction using FBG sensing technology. *Advances in Structural Engineering*, *16*(8), pp.1401-1409.
[2] Feng, D., Feng, M.Q., Ozer, E. and Fukuda, Y., 2015. A vision-based sensor for noncontact structural displacement measurement. *Sensors*, *15*(7), pp.16557-16575.
[3] Fukuda, Y., Feng, M.Q. and Shinozuka, M., 2010. Cost-effective vision-based system for monitoring dynamic response of civil engineering structures. *Structural Control and Health Monitoring*, *17*(8), pp.918-936.
[4] Fukuda, Y., Feng, M.Q., Narita, Y., Kaneko, S.I. and Tanaka, T., 2013. Vision-based displacement sensor for monitoring dynamic response using robust object search algorithm. *IEEE Sensors Journal*, *13*(12), pp.4725-4732.
[5] Ribeiro, D., Calçada, R., Ferreira, J. and Martins, T., 2014. Non-contact measurement of the dynamic displacement of railway bridges using an advanced video-based system. *Engineering Structures*, *75*, pp.164-180.
[6] Gentile, C. and Bernardini, G., 2010. An interferometric radar for non-contact measurement of deflections on civil engineering structures: laboratory and full-scale tests. *Structure and Infrastructure Engineering*, *6*(5), pp.521-534.
[7] Nassif, H.H., Gindy, M. and Davis, J., 2005. Comparison of laser Doppler vibrometer with contact sensors for monitoring bridge deflection and vibration. *Ndt & E International*, *38*(3), pp.213-218.
[8] Casciati, F. and Fuggini, C., 2011. Monitoring a steel building using GPS sensors. *Smart Structures and Systems*, *7*(5), pp.349-363.
[9] Koch, C., Georgieva, K., Kasireddy, V., Akinci, B. and Fieguth, P., 2015. A review on computer vision based defect detection and condition assessment of concrete and asphalt civil infrastructure. *Advanced Engineering Informatics*, *29*(2), pp.196-210.
[10] Prasanna, P., Dana, K., Gucunski, N. and Basily, B., 2012, April. Computer-vision based crack detection and analysis. In *Sensors and smart structures technologies for civil, mechanical, and aerospace systems 2012* (Vol. 8345, p. 834542). International Society for Optics and Photonics.
[11] Li, R., Yuan, Y., Zhang, W. and Yuan, Y., 2018. Unified vision-based methodology for simultaneous concrete defect detection and geolocalization. *Computer-Aided Civil and Infrastructure Engineering*, *33*(7), pp.527-544.